

Article

# Understanding the Photo- and Electro-Carboxylation of *o*-Methylbenzophenone with Carbon Dioxide

Keyi Tian, Ruonan Chen, Jiafang Xu, Ge Yang, Xintong Xu and Yanhua Zhang \* 

Institute of Advanced Synthesis and School of Chemistry and Molecular Engineering, Nanjing Tech University, Nanjing 211816, China; tiankeyi@njtech.edu.cn (K.T.); rnchen@njtech.edu.cn (R.C.); jiafang\_xu0611@163.com (J.X.); yangge05@njtech.edu.cn (G.Y.); xuxintong@njtech.edu.cn (X.X.)

\* Correspondence: ias\_yhzhang@njtech.edu.cn; Tel.: +86-025-58130049

Received: 31 May 2020; Accepted: 8 June 2020; Published: 12 June 2020



**Abstract:** The lack of understanding of the radical reaction mechanism of Carbon dioxide (CO<sub>2</sub>) in photo- and electro-catalysis results in the development of such applications far behind the traditional synthesis methods. Using methylbenzophenone as the model, we clarify and compare the photo-enolization/Diels–Alder (PEDA) mechanism for photo-carboxylation and the two-step single-electron reduction pathway for electro-carboxylation with CO<sub>2</sub> through careful control experiments. The regioselective carboxylation products, *o*-acylphenylacetic acid and  $\alpha$ -hydroxycarboxylic acid are obtained, respectively, in photo- and electro-chemistry systems. On the basis of understanding the mechanism, a one-pot step-by-step dicarboxylation of *o*-methylbenzophenone is designed and conducted. Both the experimental results and related density functional theory (DFT) calculation verify the feasibility of the possible pathway in which electro-carboxylation is conducted right after photo-carboxylation in one vessel. This synthesis approach may provide a mild, eco-friendly strategy for the production of polycarboxylic acids in industry.

**Keywords:** photocatalysis; electrocatalysis; photoelectro-chemistry; CO<sub>2</sub> reduction; methylbenzophenone

## 1. Introduction

CO<sub>2</sub> is one of the main components of greenhouse gases resulting from fossil fuel combustion [1]. Researchers have made lots of efforts to convert renewable CO<sub>2</sub> to high value-added chemicals, so as to reduce CO<sub>2</sub> content in the atmosphere and achieve the recycling of carbon resources [2–4]. As a thermodynamically stable molecule, CO<sub>2</sub> is usually difficult to be activated under mild conditions. Therefore, the chemical transformation of CO<sub>2</sub> is relatively challenging. While CO<sub>2</sub> is usually converted to small fuel molecules (e.g., CO, CH<sub>4</sub> and CH<sub>3</sub>OH) [5–8], it can also be used as a C1 building block to form new C–C or C–N bonds with organic molecules and eventually produce more complicated chemical feedstocks [9–12]. Considering the use of strong reducing reagents, metal catalysts or harsh reaction conditions in the traditional fixation of CO<sub>2</sub> into organic compounds, the development of mild but efficient synthesis methods becomes more attractive to researchers [13,14].

In recent years, the photochemistry and electrochemistry of CO<sub>2</sub> have developed rapidly [15–17]. With the help of light energy or electricity energy, the electron transfer dynamics of CO<sub>2</sub> are modified under mild conditions, so that the reducing agent or extra catalyst is not necessary [18,19]. However, the study of CO<sub>2</sub> in such photo- and electro-catalysis is still far behind other types of synthesis methods, and a slow reaction rate or poor selectivity is often observed. The basic reason is possibly due to the lack of understanding of related reaction mechanisms [20,21].

Among the reported organic molecules reacting with CO<sub>2</sub> under electrochemistry and photochemistry conditions (e.g., halides, olefins, alkynes, and ketones), the reaction mechanism

for methylbenzophenone has been relatively well studied. Murakami first proposed the possible mechanism for the photo-carboxylation of *o*-methylbenzophenone with CO<sub>2</sub> in 2015, as the photo-enolization/Diels–Alder (PEDA) pathway [22]. The key intermediate is the singlet dienol *E*-isomer, which is trapped with CO<sub>2</sub> via the Diels–Alder cycloaddition to afford the enol-lactone. However, Su suggested an eight-membered ring transition state theory for this process in 2016, describing a direct CO<sub>2</sub> addition to the dienol *Z*-isomer to afford the keto-carboxylic acid [23]. Afterwards, Coote conducted a theoretical calculation and figured out that Murakami's mechanism is more reasonable [24]. However, it is noted that the photoelectro-carboxylation of unsubstituted benzophenone with CO<sub>2</sub> gave an  $\alpha$ -hydroxycarboxylic acid product, following a two-step single-electron radical pathway [25]. When *o*-methylbenzophenone is applied in the above photoelectro-chemical system, a mixture of *o*-acylphenylacetic acid and  $\alpha$ -hydroxycarboxylic acid is obtained. Further study indicates that only the carbonyl site is carboxylated if there is no light irradiation involved. It is interesting that *o*-methylbenzophenone exhibits totally different regioselectivity in photo- and electro-chemistry systems, although both follow the radical mechanism. Obviously, there is no external electron participating in the photo-process, while two electrons from the power source are incorporated into the substrate during the electro-process. Thus, the actual reaction pathways for the above processes attracted our attention. We believe the understanding of such issues will facilitate the design of tunable ketone carboxylation.

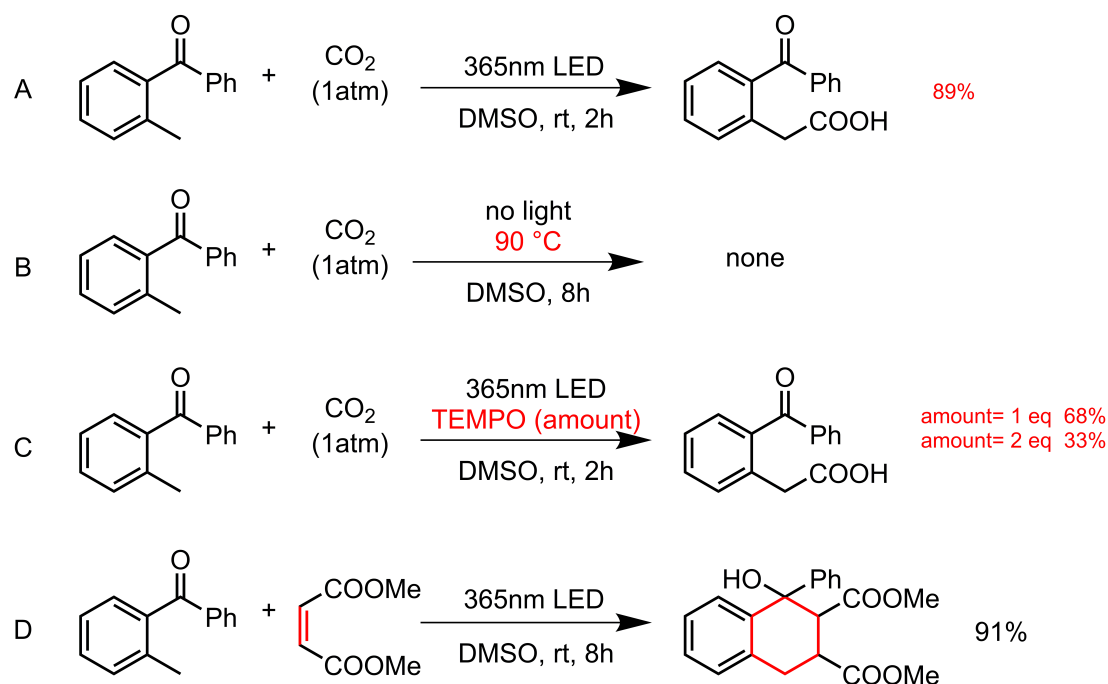
Herein, we investigate and compare the possible radical mechanisms of photo- and electro-carboxylation with CO<sub>2</sub>, using methylbenzophenone as the model. Through control experiments, the conceivable pathways are confirmed and clarified. On the basis of understanding the mechanism, one-pot synthesis of dicarboxylated *o*-methylbenzophenone is proposed and conducted. The feasibility of a different experimental protocol is discussed and further verified by certain theoretical calculation.

## 2. Results and Discussion

### 2.1. Photo-Carboxylation of Methylbenzophenone with CO<sub>2</sub>

Photo-carboxylation of *o*-methylbenzophenone with CO<sub>2</sub> (Scheme 1A, 89% yield) follows the PEDA pathway as the literature reported. This mechanism is further confirmed by our supplementary control experiments. First of all, the possible thermal effect from the strong light irradiation is eliminated since no product is observed when heating the reaction solution at 90 °C without light (Scheme 1B). The addition of a radical quencher (2,2,6,6-tetramethylpiperidinoxy, TEMPO) significantly suppresses the radical process (Scheme 1C, 68% and 33% yield when 1 eq. and 2 eq. are applied, respectively). The presence of the key dienol intermediate is also confirmed by the reaction with dimethyl maleate as a typical dienophile (Scheme 1D) [26].

When UV light is replaced by a xenon lamp (full wavelength), the reaction efficiency is significantly reduced, with the conversion yield dramatically decreasing from 98% to 35% (Table 1, entry 1 and 2). It may be ascribed to the intensity of the light sources. Certainly, the reaction does not proceed at all in the absence of light (Table 1, entry 3). In addition to the reported dimethyl sulfoxide (DMSO) (Table 1, entry 1), more solvents commonly used in photoreaction are tried. The results show that the conversion yield reaches up to 94% in *N,N*-dimethylacetamide (DMA) as a polar protic solvent (Table 1, entry 4). However, when a less polar and aprotic solvent (i.e., acetonitrile (ACN)) is applied, the product is not the desired structure, but benzo-cyclobutenol (a quaternary ring product) (Table 1, entry 5). In toluene and dichloromethane (DCM) with much lower polarity (Table 1, entry 6 and 7), the conversion of the substrate is less than 30% and the desired product yield is quite poor. Obviously, the higher the solvent polarity, the higher the conversion yield and desired product yield. The possible explanation is due to the high electron transfer rate in polar solvents.



**Scheme 1.** Photo-carboxylation of *o*-methylbenzophenone with CO<sub>2</sub> (A) under standard condition, (B) with heating instead of light, (C) with radical quencher added, and (D) reaction of *o*-methylbenzophenone with traditional dienophile.

**Table 1.** Photo-carboxylation of *o*-methylbenzophenone with CO<sub>2</sub> <sup>a</sup>.

Entry	Deviation from Standard Condition	Conversion [%] <sup>b</sup>	Yield [%] <sup>c</sup>
1	None (2 h) <sup>d</sup>	98 (98)	91 (89)
2	Xe Light (100 mW/cm <sup>2</sup> )	35	18
3	No Light	0	0
4	DMA	94	51
5	ACN	62	trace
6	Toluene	27	11
7	DCM	4	1

<sup>a</sup> Reaction solution contains *o*-methylbenzophenone (0.8 mmol) in dimethyl sulfoxide (DMSO) (20 mL) with CO<sub>2</sub> bubbling. <sup>b</sup> Conversion yield by high performance liquid chromatography (HPLC) analysis. <sup>c</sup> Isolated yield of desired product. <sup>d</sup> Reaction time is 2 h.

For *m*- and *p*-methylbenzophenone, there should be no photo-carboxylation occurring CO<sub>2</sub> due to the impossible formation of the key conjugated diene intermediate. It is confirmed by the experimental results, while most of the substrate is converted to some unknown structures in polar solvents (Supplementary Materials Figure S1). Those products are not stable even at low temperatures, but it can be recognized from the nuclear magnetic resonance (NMR) spectra that the methyl substituent does not change.

## 2.2. Electro-Carboxylation of Methylbenzophenone with CO<sub>2</sub>

For the electro-carboxylation of *o*-methylbenzophenone with CO<sub>2</sub>, basic electrochemical information of the substrate is firstly obtained through cyclic voltammetry (CV) analysis on a

glassy carbon electrode. Under Argon, a two-electron, step-by-step reduction curve is observed for *o*-methylbenzophenone (Figure 1, black trace). The reversible potential of the first electron reduction is  $-1.45$  V (all voltages are relative to the reference electrode of Ag/AgBr, unless otherwise noted). The second electron reduction is close to quasi-reversible. With CO<sub>2</sub> bubbling (Figure 1, red trace), an irreversible reduction peak appeared at  $-1.77$  V and the current density was relatively enhanced, suggesting that CO<sub>2</sub> reacted with the radical intermediates generated from *o*-methylbenzophenone to form a quite stable structure. In addition, the onset potential of the substrate is slightly more positive (ca. 0.08 V) with CO<sub>2</sub> bubbling than under argon, which may be due to the rapid reaction between CO<sub>2</sub> and free radical anions.

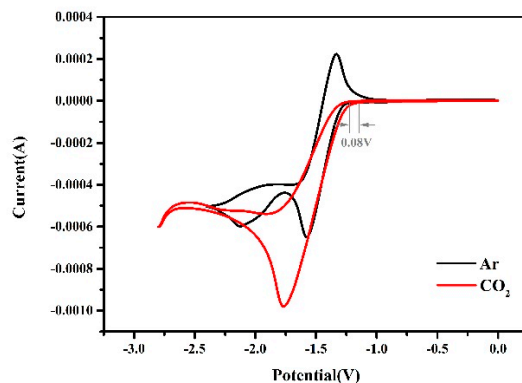


**Figure 1.** Cyclic voltammogram of *o*-methylbenzophenone on a glassy carbon (GC) electrode under argon (black trace) or with CO<sub>2</sub> bubbling (red trace). The reaction solution consists of supporting electrolyte (0.1 M of Bu<sub>4</sub>NBr) and *o*-methylbenzophenone (40.0 mM) in 20 mL of acetonitrile by using Ag/AgBr as the reference electrode and Al as the counter electrode.

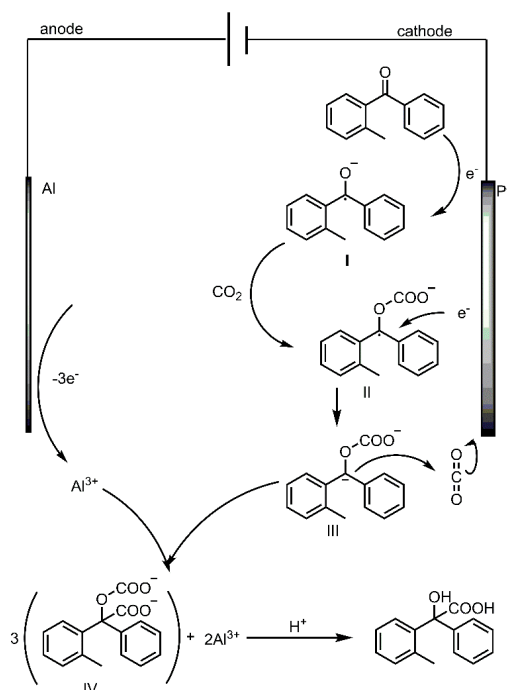
The product of the above electro-carboxylation of *o*-methylbenzophenone with CO<sub>2</sub> is determined to be 2-hydroxy-2-(2-methylphenyl)-2-phenyl-acetic acid. The carboxylation occurs on the carbonyl carbon instead of the methyl group, completely different from the photo-carboxylation process. Further study indicates that different working electrodes have certain effects on the reaction efficiency. Among glassy carbon electrodes, fluorinated tin oxide (FTO) electrodes, platinum electrodes and gold-nickel foam electrodes, the performance of platinum electrodes is much better and is applied as the working electrode in our further investigation. On the basis of CV analysis, the suitable applied voltage is investigated around  $-1.7$  V. It is noted that the reaction hardly occurs at  $-1.4$  V (Table 2, entry 1), while the product is obtained with a 36% yield at  $-1.5$  V (Table 2, entry 2). With the increase in applied potential, the conversion yield increases gradually (Table 2, entry 3–5). The good reaction efficiency is obtained at  $-1.8$  V with an up to 94% conversion yield and 88% product yield (Table 2, entry 5). Afterwards, more by-products are formed at a higher potential while the desired product yield drops (Table 2, entry 6). Moreover, besides ACN, DMSO (Table 2, entry 7) and DMA (Table 2, entry 8) are also good solvents for this electro-carboxylation process. Thus, the polarity of the solvent does not affect the electro-carboxylation process as significantly as the photo-carboxylation process. It is possible that the uniform dispersion of the supporting electrolyte in the electrochemical system weakens the solvent's influence on the electron transfer efficiency in the solution [27]. When light irradiation is applied in this system, the substrate is almost consumed, but a mixture of  $\alpha$ -hydroxycarboxylic acid and *o*-acylphenylacetic acid is obtained, while a few dicarboxylated products are observed (Table 2, entry 9 and 10). Further study indicates that the photo-carboxylation product is easy to generate as long as light is involved (low to 30 mW/cm<sup>2</sup>), even if a higher potential is applied ( $-2.5$  V or  $-15$  mA/cm<sup>2</sup>). It is speculated that the activation energy for the photo-carboxylation pathway is much lower than that for the electro-carboxylation pathway.

**Table 2.** Electro-carboxylation of *o*-methylbenzophenone with CO<sub>2</sub> <sup>a</sup>.

Entry.	Deviation from Standard Condition	Conversion [%] <sup>b</sup>	Yield [%] <sup>c</sup>
1	-1.4 V	trace	not available
2	-1.5 V	43	36
3	-1.6 V	52	44
4	-1.7 V	74	62
5	None	94	88
6	-1.9 V	98	25
7	DMSO	90	78
8	DMA	90	76
9	Xe light (30 mW/cm <sup>2</sup> )	95 (26) <sup>d</sup>	68
10	Xe light (300 mW/cm <sup>2</sup> )	99 (84) <sup>d</sup>	14

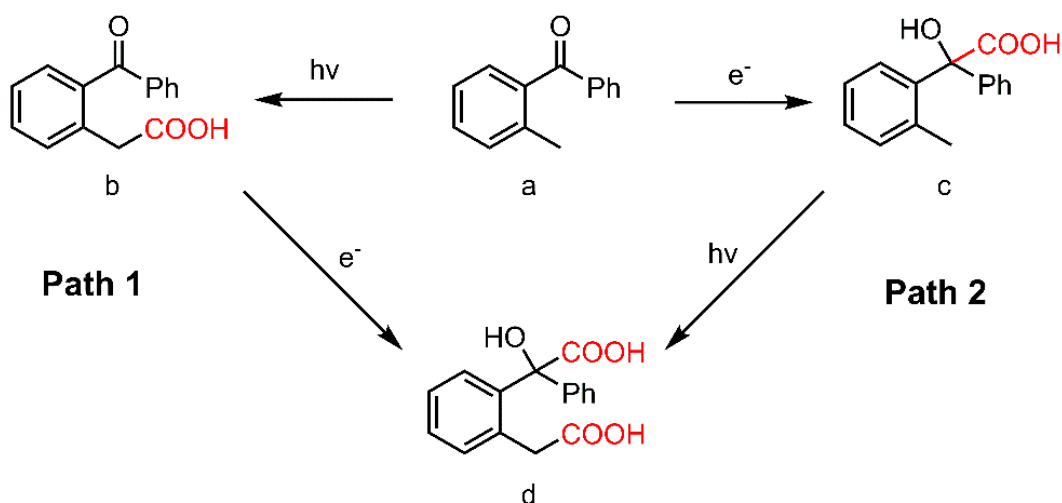
<sup>a</sup> Reaction conditions: *o*-methylbenzophenone (0.8 mmol) and Bu<sub>4</sub>NBr (2.0 mmol) in acetonitrile (ACN) (20 mL) with CO<sub>2</sub> bubbling, Al as the anode and Ag/AgBr as the reference electrode. <sup>b</sup> Conversion yield by HPLC analysis. <sup>c</sup> Isolated yield of desired product. <sup>d</sup> Yield of *o*-acylphenylacetic acid (photo-carboxylation product) by HPLC.

The electro-carboxylation of *m*- and *p*-methylbenzophenone with CO<sub>2</sub> (Supplementary Materials Figure S2) is also screened. As expected, both of the carboxylations occur at the carbonyl site. Since the only product of the above electro-carboxylation is hydroxycarboxylic acid, the possible mechanism may consist of a two-step single-electron transfer process (Scheme 2), similar to Wang's mechanism. *o*-Methylbenzophenone obtains one electron from the cathode and the C=O bond is reduced to the radical anion I. After one CO<sub>2</sub> fixation to form the carboxylic acid radical anion II, the second electron is incorporated to produce the carboxylic acid anion III, followed by another CO<sub>2</sub> addition to form the carboxylate anion IV. After acidification, the desired hydroxycarboxylic acid product is obtained.

**Scheme 2.** Proposed mechanism for electro-carboxylation of *o*-methylbenzophenone with CO<sub>2</sub>.

### 2.3. Dicarboxylation of *o*-Methylbenzophenone with CO<sub>2</sub>

On the basis of understanding the possible mechanism of electro- and photo-carboxylation, the dicarboxylation of *o*-methylbenzophenone with CO<sub>2</sub> through photoelectro-chemistry naturally comes into our consideration. As mentioned above (Table 2, entry 9 and 10), a few dicarboxylated products are observed when light and potential are applied simultaneously. There are two possible pathways in this transformation. One is the electro-carboxylation of photo-carboxylated product (Scheme 3, path 1), and another is just changing the order (Scheme 3, path 2). In terms of the photo-carboxylation mechanism, path 2 is less likely to succeed, since the key dienol intermediate could not be formed from  $\alpha$ -hydroxycarboxylic acid (Scheme 3, compound c). The experimental results further confirm this assumption. Thus, the more feasible path 1 becomes the basis of our design for the dicarboxylation process.



**Scheme 3.** Dicarboxylation of *o*-methylbenzophenone with CO<sub>2</sub>.

Due to the poor efficiency of synchronous photo- and electro-carboxylation, a one-pot step-by-step dicarboxylation procedure is proposed. That is, the photo-carboxylation and subsequent electro-carboxylation are conducted in one vessel. From the CV analysis (Supplementary Materials Figure S3) of *o*-acylphenylacetic acid (Scheme 3, compound b), it is noted that its onset potential is at  $-1.4$  V and the reduction peak at  $-2.2$  V, which is ca.  $0.5$  V more negative than *o*-methylbenzophenone. That means higher electric energy would be consumed in this electrochemical process. In fact, a constant current of  $-15$  mA/cm<sup>2</sup> is necessary during this electro-carboxylation. Considering the performance of solvents in both photo- and electro-carboxylation, DMSO is relatively suitable for this process. Finally, a dicarboxylic acid, 2-(2-(carboxymethyl)-phenyl)-2-hydroxy-2-phenylacetic acid (Scheme 3, compound d), is obtained in this one-pot approach, confirmed by liquid chromatography—mass spectrometry (LC-MS) analysis.

The corresponding density functional theory (DFT) calculation for the electro-carboxylation step in path 1 is conducted to indicate the possible thermodynamics (Figure 2 (for details, please see Supplementary Materials)) [28–35]. It is noted that the energy barriers for two successive CO<sub>2</sub> additions are only  $9.4$  and  $8.1$  kcal/mol, respectively. This shows the reaction may proceed smoothly. For the intermediate structure im5, the singlet is much more stable than the triplet with ca.  $36$  kcal/mol of energy difference, which means the actual reaction should occur at the singlet state.

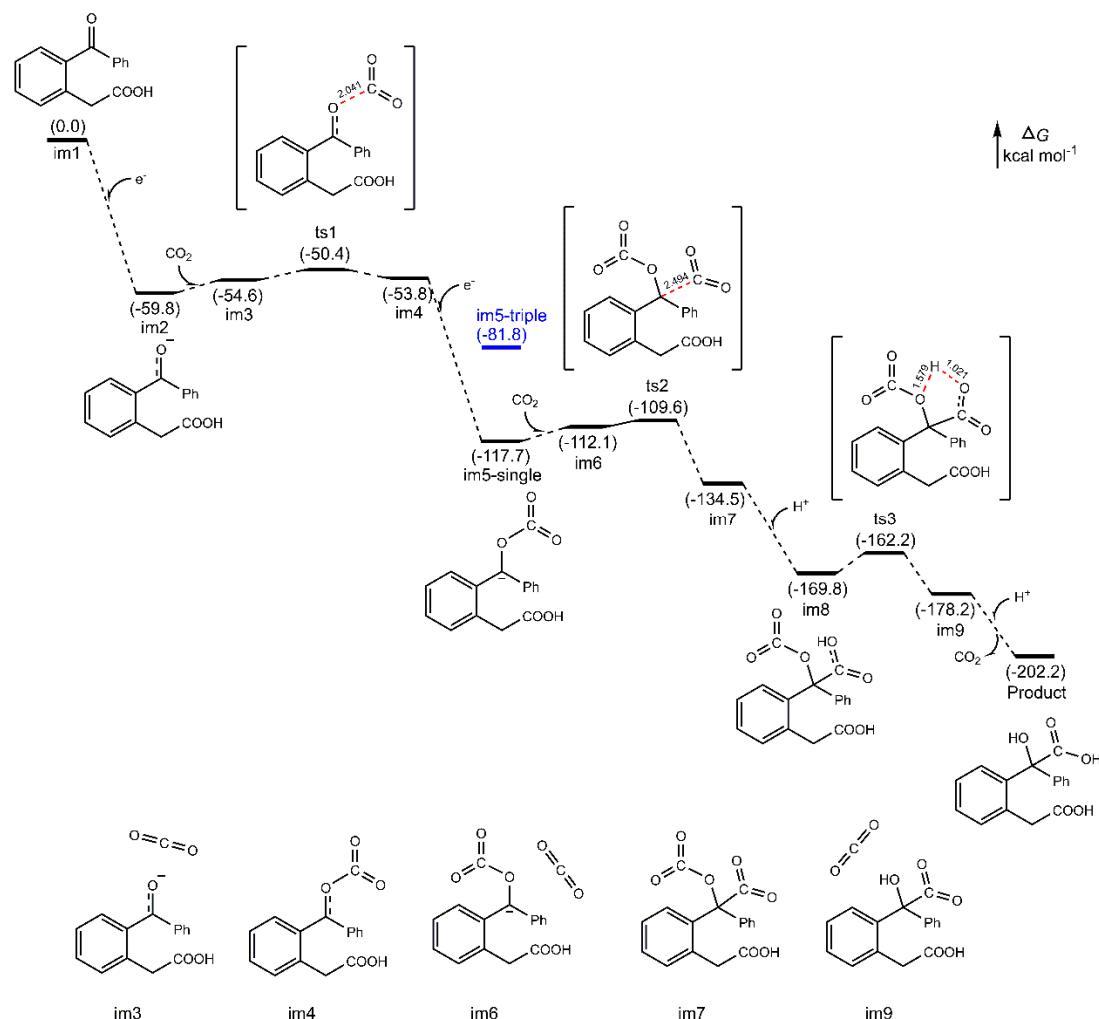


**Figure 2.** Energy profiles for the electro-carboxylation of *o*-acylphenylacetic acid. The relative Gibbs energies are given in kcal mol<sup>-1</sup>, at 298 K, 1 atm. All the geometries are optimized in DMSO solvent at the M062X/6-311+G(d) level based on the polarized continuum model (SMD). The bonding length is reported in Å.

### 3. Materials and Methods

*o*-Methylbenzophenone (Aladdin), *m*-methylbenzophenone (Alfa Aesar), *p*-methylbenzophenone (Aladdin), tetrabutylammonium bromide and CO<sub>2</sub> (99.9%) were purchased and used without further treatment. Dimethyl sulfoxide, acetonitrile and *N,N*-dimethyl acetyl were super dried with a molecular sieve. All other reagents and solvents, unless otherwise noted, were purchased from commercial vendors and used without further purification.

#### 3.1. Photo-Carboxylation of *o*-Methylbenzophenone

The solution of *o*-Methylbenzophenone (156.8 mg, 0.80 mmol) in dimethyl sulfoxide (20 mL) was irradiated by a LED lamp (365 nm) under a CO<sub>2</sub> atmosphere. Upon reaction completion, water was added and the mixture was extracted with ethyl acetate (5 × 10 mL). The combined organic layer was washed with NaOH aq. (5 × 10 mL). Then, the combined aqueous phase was acidified with 2.0 M of HCl aq. (5 mL), followed by an extraction with ethyl acetate (5 × 10 mL). The organic phase was washed with brine and dried over Na<sub>2</sub>SO<sub>4</sub>. The solvent was removed under reduced pressure to afford the carboxylic acid product. The photo-carboxylation of *m*-methylbenzophenone and *p*-methylbenzophenone followed procedures similar to above.

### 3.2. Electro-Carboxylation of *o*-Methylbenzophenone

*o*-Methylbenzophenone (156.8 mg, 0.80 mmol), tetrabutylammonium bromide (0.644 g, 2.00 mmol) and acetonitrile (20 mL) were added in a three-necked flask under Ar before assembling a three-electrode electrochemistry system with a platinum sheet as the working electrode, Al foil as the counter electrode and Ag/AgBr as the reference electrode. CO<sub>2</sub> was bubbled into the vessel continuously at a controlled flow rate for several minutes to saturate the solution, then a suitable potential was applied to the reaction mixture with vigorous stirring. After the reaction was complete, the crude mixture was concentrated in vacuo and quenched with 1 N HCl aq. (2.0 mL), followed by extraction with ethyl acetate (3 × 20 mL). The combined organic layer was dried over anhydrous MgSO<sub>4</sub>, filtered and concentrated in vacuo to afford the crude product. After purification on column chromatography (Hexane/Ethyl acetate), a pure product was isolated.

### 3.3. One-Pot Photoelectro-Dicarboxylation of *o*-Methylbenzophenone

*o*-Methylbenzophenone (156.8 mg, 0.80 mmol) was charged in a three-necked flask equipped with the working electrode (Pt), the reference electrode (Ag/AgBr) and the counter electrode (Al), which was subsequently filled with CO<sub>2</sub>. Dimethyl sulfoxide (20 mL) was added, and then the reaction mixture was irradiated with a LED lamp (365 nm). After 8 h, the light was removed and a strong voltage (constant current −15 mA/cm<sup>2</sup>) was applied. After 24 h, water was added to quench the reaction and the mixture was extracted with ethyl acetate (5 × 10 mL). The combined organic layer was washed with NaOH aq. (5 × 10 mL). Then, the combined aqueous layer was acidified with 2.0 M of HCl aq. (5 mL) and extracted with ethyl acetate (5 × 10 mL). The collected organic phase was washed with brine and dried over Na<sub>2</sub>SO<sub>4</sub>. The solvent was removed under reduced pressure to afford a mixture of acid products, which was further analyzed by LC-MS.

## 4. Conclusions

In conclusion, the photo-carboxylation of *o*-methylbenzophenone with CO<sub>2</sub> follows the photo-enolization/Diels–Alder mechanism as reported, while electro-carboxylation follows a two-step single-electron reduction pathway. The regioselective carboxylation products, *o*-acylphenylacetic acid and  $\alpha$ -hydroxycarboxylic acid, are obtained, respectively, in photo- and electro-chemistry systems. The factors affecting the reaction are investigated and the competitive relationship between these two radical mechanisms is discussed. It is observed that photo-carboxylation proceeds much more smoothly than electro-carboxylation, meaning a lower energy barrier in the photo-radical pathway. On the basis of understanding both mechanisms, a one-pot dicarboxylation of *o*-methylbenzophenone is designed and successfully conducted in the order of photo-carboxylation and then electro-carboxylation in one reaction vessel. The corresponding theoretical calculation also supports the feasibility of this pathway by thermodynamics analysis. This synthesis method provides a new eco-friendly strategy for the production of polycarboxylic acids in industry. Furthermore, with the help of a theoretical calculation to predict the possible structure and reaction pathway, we are encouraged to design and synthesize more complicated compounds in the future.

**Supplementary Materials:** The following are available online at <http://www.mdpi.com/2073-4344/10/6/664/s1>, Equipments, Characterization data and spectra of compounds, Figure S1: Photo-carboxylation of *o*-, *m*- and *p*-methylbenzophenone with CO<sub>2</sub> in different solvent, Figure S2: Electro-carboxylation of *o*-, *m*- and *p*-methylbenzophenone with CO<sub>2</sub> in different solvent, Figure S3: Cyclic voltammogram of a) *o*-methylbenzophenone and b) *o*-acylphenylacetic acid on glassy carbon electrode under argon (black trace) or with CO<sub>2</sub> bubbling (red trace), DFT data.

**Author Contributions:** Conceptualization, K.T., R.C., G.Y. and Y.Z.; Formal analysis, K.T.; Investigation, K.T.; Software, K.T., J.X. and X.X.; Supervision, Y.Z.; Writing—original draft, K.T.; Writing—review and editing, Y.Z. All authors have read and agreed to the published version of the manuscript.

**Funding:** The authors thank National Natural Science Foundation of China (No. 21673117 and 91956109), Jiangsu Provincial Foundation for Specially-Appointed Professor, and Start-up Fund from Nanjing Tech University (No. 39837126 and 39837102).

**Conflicts of Interest:** The authors declare no conflict of interest. The funders had no role in the design of the study; in the collection, analyses, or interpretation of data; in the writing of the manuscript, or in the decision to publish the results.

## References

1. Bushuyev, O.S.; De Luna, P.; Cao, T.D.; Tao, L.; Saur, G.; van de Lagemaat, J.; Kelley, S.O.; Sargent, E.H. What Should We Make with CO<sub>2</sub> and How Can We Make It? *Joule* **2018**, *2*, 825–832. [[CrossRef](#)]
2. Dindi, A.; Dang, V.Q.; Vega, L.F.; Nashef, E.; Abu-Zahra, M.R.M. Applications of fly ash for CO<sub>2</sub> capture, utilization, and storage. *J. CO<sub>2</sub> Util.* **2019**, *29*, 82–102. [[CrossRef](#)]
3. Xie, Z.; Zhang, X.; Zhang, Z.; Zhou, Z. Metal-CO<sub>2</sub> Batteries on the Road: CO<sub>2</sub> from Contamination Gas to Energy Source. *Adv. Mater.* **2017**, *29*, 1605891. [[CrossRef](#)] [[PubMed](#)]
4. Frontera, P.; Macario, A.; Ferraro, M.; Antonucci, P. Supported Catalysts for CO<sub>2</sub> Methanation: A Review. *Catalysts* **2017**, *7*, 59. [[CrossRef](#)]
5. Ji, L.; Li, L.; Ji, X.; Zhang, Y.; Mou, S.; Wu, T.; Liu, Q.; Li, B.; Zhu, X.; Luo, Y.; et al. Highly Selective Electrochemical Reduction of CO<sub>2</sub> to Alcohols on an FeP Nanoarray. *Angew. Chem. Int. Ed.* **2020**, *59*, 758–762. [[CrossRef](#)] [[PubMed](#)]
6. Fernandez, S.; Franco, F.; Casadevall, C.; Martin-Diaconescu, V.; Luis, J.M.; Lloret-Fillol, J. A Unified Electro- and Photocatalytic CO<sub>2</sub> to CO Reduction Mechanism with Aminopyridine Cobalt Complexes. *J. Am. Chem. Soc.* **2020**, *142*, 120–133. [[CrossRef](#)]
7. Zheng, T.; Jiang, K.; Wang, H. Recent Advances in Electrochemical CO<sub>2</sub>-to-CO Conversion on Heterogeneous Catalysts. *Adv. Mater.* **2018**, *30*, 1802066. [[CrossRef](#)]
8. Dabral, S.; Schaub, T. The Use of Carbon Dioxide (CO<sub>2</sub>) as a Building Block in Organic Synthesis from an Industrial Perspective. *Adv. Synth. Catal.* **2019**, *361*, 223–246. [[CrossRef](#)]
9. Yang, Z.Z.; He, L.N.; Gao, J.; Liu, A.H.; Yu, B. Carbon dioxide utilization with C-N bond formation: Carbon dioxide capture and subsequent conversion. *Energy Environ. Sci.* **2012**, *5*, 6602–6639. [[CrossRef](#)]
10. Hong, J.; Li, M.; Zhang, J.; Sun, B.; Mo, F. C-H Bond Carboxylation with Carbon Dioxide. *ChemSuschem* **2019**, *12*, 6–39. [[CrossRef](#)]
11. Borjesson, M.; Moragas, T.; Gallego, D.; Martin, R. Metal-Catalyzed Carboxylation of Organic (Pseudo)halides with CO<sub>2</sub>. *ACS. Catal.* **2016**, *6*, 6739–6749. [[CrossRef](#)] [[PubMed](#)]
12. Kamphuis, A.J.; Picchioni, F.; Pescarmona, P.P. CO<sub>2</sub>-fixation into cyclic and polymeric carbonates: Principles and applications. *Green Chem.* **2019**, *21*, 406–448. [[CrossRef](#)]
13. Yaashikaa, P.R.; Kumar, P.S.; Varjani, S.J.; Saravanan, A. A review on photochemical, biochemical and electrochemical transformation of CO<sub>2</sub> into value-added products. *J. CO<sub>2</sub> Util.* **2019**, *33*, 131–147. [[CrossRef](#)]
14. Takeda, H.; Cometto, C.; Ishitani, O.; Robert, M. Electrons, Photons, Protons and Earth-Abundant Metal Complexes for Molecular Catalysis of CO<sub>2</sub> Reduction. *ACS. Catal.* **2017**, *7*, 70–88. [[CrossRef](#)]
15. Yeung, C.S. Photoredox Catalysis as a Strategy for CO<sub>2</sub> Incorporation: Direct Access to Carboxylic Acids from a Renewable Feedstock. *Angew. Chem. Int. Ed.* **2019**, *58*, 5491–5502. [[CrossRef](#)] [[PubMed](#)]
16. Wu, J.; Huang, Y.; Ye, W.; Li, Y. CO<sub>2</sub> Reduction: From the Electrochemical to Photochemical Approach. *Adv. Sci.* **2017**, *4*, 1700194. [[CrossRef](#)] [[PubMed](#)]
17. Doherty, A.P.; Marley, E.; Barhdadi, R.; Puchelle, V.; Wagner, K.; Wallace, G.G. Mechanism and kinetics of electrocarboxylation of aromatic ketones in ionic liquid. *J. Electroanal. Chem.* **2018**, *819*, 469–473. [[CrossRef](#)]
18. Duan, X.; Xu, J.; Wei, Z.; Ma, J.; Guo, S.; Wang, S.; Liu, H.; Dou, S. Metal-Free Carbon Materials for CO<sub>2</sub> Electrochemical Reduction. *Adv. Mater.* **2017**, *29*, 1701784. [[CrossRef](#)]
19. Trickett, C.A.; Helal, A.; Al-Maythaly, B.A.; Yamani, Z.H.; Cordova, K.E.; Yaghi, O.M. The chemistry of metal-organic frameworks for CO<sub>2</sub> capture, regeneration and conversion. *Nat. Rev. Mater.* **2017**, *2*, 17045. [[CrossRef](#)]
20. Xu, S.; Carter, E.A. Theoretical Insights into Heterogeneous (Photo)electrochemical CO<sub>2</sub> Reduction. *Chem. Rev.* **2019**, *119*, 6631–6669. [[CrossRef](#)]
21. Gao, D.; Aran-Ais, R.M.; Jeon, H.S.; Roldan, C.B. Rational catalyst and electrolyte design for CO<sub>2</sub> electroreduction towards multicarbon products. *Nat. Catal.* **2019**, *2*, 198–210. [[CrossRef](#)]
22. Masuda, Y.; Ishida, N.; Murakami, M. Light-Driven Carboxylation of o-Alkylphenyl Ketones with CO<sub>2</sub>. *J. Am. Chem. Soc.* **2015**, *137*, 14063–14066. [[CrossRef](#)] [[PubMed](#)]

23. Su, S.H.; Su, M.D. Mechanistic analysis of the photochemical carboxylation of o-alkylphenyl ketones with carbon dioxide. *RSC Adv.* **2016**, *6*, 50825–50832. [[CrossRef](#)]
24. Blyth, M.T.; Noble, B.B.; Russell, I.C.; Coote, M.L. Oriented Internal Electrostatic Fields Cooperatively Promote Ground- and Excited-State Reactivity: A Case Study in Photochemical CO<sub>2</sub> Capture. *J. Am. Chem. Soc.* **2020**, *142*, 606–613. [[CrossRef](#)] [[PubMed](#)]
25. Liu, R.; Yuan, G.; Joe, C.L.; Lightburn, T.E.; Tan, K.L.; Wang, D. Silicon Nanowires as Photoelectrodes for Carbon Dioxide Fixation. *Angew. Chem. Int. Ed.* **2012**, *51*, 6709–6712. [[CrossRef](#)]
26. Javier, M.; Alessio, C.C.; Tommaso, C.; Marcella, B.; Nadia, M.; Xavier, C.; Luca, A.A. A microfluidic photoreactor enables 2-methylbenzophenone light-driven reactions with superior performance. *Chem. Commun.* **2018**, *54*, 6820–6823.
27. Isse, A.A.; Galia, A.; Belfiore, C.; Silvestri, G.; Gennaro, A. Electrochemical reduction and carboxylation of halobenzophenones. *J. Electroanal. Chem.* **2002**, *526*, 41–52. [[CrossRef](#)]
28. Frisch, M.J.; Trucks, G.W.; Schlegel, H.B.; Scuseria, G.E.; Robb, M.A.; Cheeseman, J.R.; Scalmani, G.; Barone, V.; Mennucci, B.; Petersson, G.A.; et al. *Gaussian 09 (Revision D.01)*; Gaussian, Inc.: Wallingford, CT, USA, 2013.
29. Zhao, Y.; Truhlar, D.G. Density functionals with broad applicability in chemistry. *Accounts Chem. Res.* **2008**, *41*, 157–167. [[CrossRef](#)]
30. Krishnan, R.; Binkley, J.S.; Seeger, R.; Pople, J.A. Self-Consistent Molecular-orbital Methods.20. Basis Set for Correlated Wave-functions. *J. Chem. Phys.* **1980**, *72*, 650–654. [[CrossRef](#)]
31. Marenich, A.V.; Cramer, C.J.; Truhlar, D.G. Universal solvation model based on solute electron density and on a continuum model of the solvent defined by the bulk dielectric constant and atomic surface tensions. *J. Phys. Chem. B* **2009**, *113*, 6378–6396. [[CrossRef](#)]
32. Gonzalez, C.; Schlegel, H.B. An Improved Algorithm for Reaction-path Following. *J. Chem. Phys.* **1989**, *90*, 2154–2161. [[CrossRef](#)]
33. Markovic, Z.; Tosovic, J.; Milenkovic, D.; Markovic, S. Revisiting the solvation enthalpies and free energies of the proton and electron in various solvents. *Comput. Theor. Chem.* **2016**, *1077*, 11–17. [[CrossRef](#)]
34. Fifen, J.J.; Dhaouadi, Z.; Nsangou, M. Revision of the Thermodynamics of the Proton in Gas Phase. *J. Phys. Chem. A* **2014**, *118*, 11090–11097. [[CrossRef](#)] [[PubMed](#)]
35. Fifen, J.J. Thermodynamics of the Electron Revisited and Generalized. *J. Chem. Theory Comput.* **2013**, *9*, 3165–3169. [[CrossRef](#)] [[PubMed](#)]



© 2020 by the authors. Licensee MDPI, Basel, Switzerland. This article is an open access article distributed under the terms and conditions of the Creative Commons Attribution (CC BY) license (<http://creativecommons.org/licenses/by/4.0/>).